

# Tactile Display Design for Securing Flight and Reducing the Saturation of Pilot's Visual Channel

Khaled Fellah and Mohamed Guiatni

*Control Laboratory, Ecole Militaire Polytechnique, Bordj El Bahri, Algiers, Algeria*

**Keywords:** Tactile Feedback, Fuzzy Logic Controller (FLC), Pilot's Visual Channel Saturation, Inverse Dynamic, Flight Simulation, Xplane, Tactors.

**Abstract:** Visual channel dominates the design of the cockpit, and auditory channel is progressively being used as well. However, tactile displays are almost abstract in the cockpit designs. Whereas, many research proved that several applications exist where the tactile displays may become an important or even essential choice. This is due to the fact that the visual feedback is not suitable, not adequate, or surcharged and that the visual attention is usually limited to a simple entity. In this paper, we propose a design of a low-cost tactile feedback system to provide the pilot with better insight in the flight path and prevent limitations during flight. In the first part of the paper, we develop an effective control strategy based on inverse dynamic to solve the problems of use of the low-cost tactors. The obtained results showed reduction of 48 % in settling time. The second part describes the use of Fuzzy Logic Controllers (FLC) to compute a new form of tactile output of the translation of a pertinent flight data information and flight envelope to vibrotactile feedback signals. And in the last part, we develop a wireless (and USB) vibrotactile feedback device consisting of 16 embedded tactors controlled with an inverse dynamic strategy via an arm Cortex M3 architecture. Pilots equipped with the developed tactile display were capable of successfully flying in a simulator. They confirm that tactile feedback is an interesting way of feeding back information about the airplane's state, in order to give a better understanding of what the airplane is doing during controlled flight.

## 1 INTRODUCTION

The human vision is a very convenient channel for processing large amounts of data because our brain receives around 80% of all information from visual cues (Rosenblum, 2011). However, a pilot interacts with the modern cockpit displays through cursor control devices (CCD) or multi-function displays (MFD), and the total quantity of information which is at the disposal of pilot is offered mainly in a visual format (Thomas et al., 2015). The problems which the developers of the human-machine interfaces encounter in the modernization of the new cockpits are primarily caused by the limit of the capacities of the pilots to process the information related to the data of flight (Van Veen and Van Erp, 2001). In addition, the excess of visual information channel can cause fatal accidents if a pilot cannot analyze or perceive stimuli at the right time (Petit, 2013). This menace of sensory overload makes the designers of cockpit progressively apply multimodal interfaces (Lloyd et al., 2003). Traditionally, the auditory display is considered as an alternative or complementary to visual dis-

plays. However, the visual and auditory channels of a pilot are sometimes strongly loaded, degraded or not available (Van Erp and Self, 2008). Several research tasks to integrate tactile display applications, in order to provide countermeasures of the spatial disorientation (SD) and solutions to the threats of the sensory and/or cognitive overload (Self et al., 2008). Application of the touch screens in the cockpits of different types of aircraft got much attention. In 2015, Salzer et al. (Salzer and Oron-Gilad, 2015) designed a tactile feedback system display on-thigh part in a cockpit to improve flight safety by improving the situational awareness of helicopter pilots and reducing the collisions probabilities. Schmidt-Skipiol (Schmidt-Skipiol, 2015) presented a new concept of the use of tactile feedback with Flight Envelope Protection. Coalition Warfare Program (CWP) (Lawson and Rupert, 2014) developed a Tactile Situation Awareness System (TSAS) on-torso in UH-60 Black Hawk. The results showed that landing performance in degraded visual environments was significantly improved when ground speed and altitude were presented on a tactile display (Jansen et al., 2008). Nojima et al. (No-

jima and Funabiki, 2005) developed a tactile display system consisting of 6x4 pin-array tactors placed on an aircraft control side-stick to inform a pilot about altitude and vertical speed and increase situational awareness during flight path. VanErp et al. (Van Erp et al., 2005) examined the possibility to present the helicopter navigation information on a belt tactile display, including the translation of distance to vibration rhythm and the direction to vibration location. McGrath (McGrath, 2000) used a tactile display of 12 tractors to demonstrate that it is possible to manually fly an airplane (T34-C) without visual instruments and outside view by feeding back the pitch and the bank angle simultaneously to the pilot. In this study, we aim to design a vibrotactile display to provide a current optimal state of the aircraft to the pilot and display the warning signal about a limitation of the flight envelope, flight path climb, pitch or bank angles limitations. A new approach is adopted by exploiting the results of the work of McGrath (McGrath, 2000) with the use of a low cost tactors. In this study, we aimed at finding quantitative and qualitative performance differences while combining a low cost tactile system with the flight envelope generating an artificial stress situation.

## 2 VIBROTACTILE DISPLAY DESIGN

### 2.1 Vibrotactile Actuators

Devices that are used to stimulate the human skin in embedded tactile display communication systems must create a range of sensations which vary according to the intensity, duration of stimulation, locus of stimulation, frequency and waveforms (Jones and Sarter, 2008). Other important engineering considerations factors generally include weight, shape, size, power consumption, cost, durability, reliability, availability, and wearability (Jones and Sarter, 2008). Two types of actuators are commonly used for tactile stimulation, electrotactile and vibrotactile, which are distinguished on the basis of the mechanism used to stimulate the human skin (Jones and Sarter, 2008). Electrotactile actuators stimulate the human skin by passing a current through surface electrodes. Vibrotactile actuators stimulate the skin by converting electrical energy into a mechanical displacement. Vibrotactile stimulation can be divided into four broad classes, piezo-actuators, Shape memory alloy (SMA), linear resonant actuators (LRAs) or eccentric rotating masses (ERMs) could be utilized

(Van Erp et al., 2005). Tactors type ERM actuators are compact and lightweight, and have a larger bandwidth than LRA actuators. Moreover, coin LRA actuators vibrate in the axial direction (i.e. normal to the coin surface) whereas coin type ERM actuators produce radial vibrations (Renwick, 2008). Brown and Kaaresoja (Brown and Kaaresoja, 2006) compared the ERM to the C2 tactors by varying the rhythm and intensity of the vibration. They found that the overall vibrotactile signal recognition of human study participants using an ERM actuator was nearly identical to the participants signal recognition using a C2 tactor (Choi and Kuchenbecker, 2013). This result is promising, as it suggests that the pager motors may provide the same performance in terms of recognizing and identifying vibratory signals as much more expensive tactors. Therefore, we have chosen the 308-102 tactors, manufactured by Precision Microdrives. These are ERM actuators which offer peak amplitude of 5.5G, with a body diameter of 8mm, and they cost less than 20 \$. However, this type of actuators presents a delay of few hundred milliseconds (Choi and Kuchenbecker, 2013). In order to overcome this problem, we have developed a inverse dynamics based controller with friction compensation.

### 2.2 System Design and Discussion

The developed tactile feedback system consists of 16 tactors placed in defined position in the skin, and a control device containing a FLC for the conversion of the flight data into tactile signal. Another controller base on dynamic inverse to modify the dynamics of the tactors to use them in the prevention from the pilotes capacities degradation.

To study and analyze the developed tactile system, a platform of tests is proposed. This tests must be near as possible as to the real conditions. For that, we implement the Hardware-in-the-Loop-Simulation (HILS) including a developed tactile display system, aircraft dynamic model and X-plane.

The model of an aircraft is implemented in Matlab/ Simulink. A series of tests on X-plane environment is performed to see the behavior of the developed model in different flight situations. As an experiment we sent the measured geodetic latitude, longitude and altitude inputs from the model to flight control surfaces of an aircraft in the X-Plane environment. The tactile display system recieved the calculated flight envelope limit, flight path climb, pitch, bank and turn rate angles and translated it into effective vibrotactile signal. Through this HIL simulation, the tactile display system can be tested on real aircraft minimizing risks.

### 2.3 Hardware-in-the-Loop Simulation

The main components of the Design of the hardware-in-the-loop simulation structure is :

- Aircraft Dynamics.
- Flight Simulator X-Plane application.
- Tactile display hardware and software system.

The pilot commands the aircraft surface in the X-plane environment by introducing inputs from the stick to the aircraft model. The flight simulator X-Plane application is used as a visualization of the aircraft movement. Thus, the objective is to establish the communication between aircraft model, X-Plane and tactile display system to visualize movement of plane and encode the flight data and warning signal into tactile signal. The aircraft model calculates position, flight envelope, flight path climb and turn rate angles according to the pilot's inputs. Tactile display hardware system communicates with computer that contains Aircraft dynamics block using USB communication or XBEE interface, while the communication between Aircraft dynamics block and Flight Simulator X-Plane application is the standard protocol UDP (User Datagram Protocol).

### 2.4 Flight Simulation Software: X-Plane

X-Plane offers the most realistic flight model that can be used to predict the flying qualities of 30 aircraft in the default installation with incredible accuracy. X-Plane is not a game, but it's an engineering tool and has the ability to send and receive flight data via User Datagram Protocol (UDP) communication. These parameters are sent by the Matlab/Simulink aircraft models in the IEEE754 format. The data needed by X-plane to visualize the movement of an aircraft in the hardware simulation is in fact the position data of the aircraft (longitude, latitude, altitude) and the attitude of aircraft (roll angle, pitch angle, and yaw angle).

The triple of states that can be sent to describe the position of an aircraft in X-plane application are geodetic latitude  $\mu$ , the geodetic longitude  $\lambda$  and the geodetic height  $h$  with respect to the ECEF-Frame and given by equation (1).

$$\begin{pmatrix} \dot{\lambda} \\ \dot{\mu} \\ \dot{h} \end{pmatrix}_O^E = \begin{pmatrix} \frac{(V_K^G)^E \sin \chi_K^G \cos \gamma_K^G}{(N_{\mu} + (h)_0^E) \cos(\mu)_0^E} \\ \frac{(V_K^G)^E \cos \chi_K^G \cos \gamma_K^G}{M_{\mu} + (h)_0^E} \\ (V_K^G)^E \sin \gamma_K^G \end{pmatrix} \quad (1)$$

Where

$$N_{\mu} = \frac{a}{\sqrt{1 - e^2 \sin^2(\mu)_0^E}}$$

$$M_{\mu} = \frac{1 - e^2}{1 - e^2 \sin^2(\mu)_0^E} \quad (2)$$

The position of a point in space is specified according to the World Geodetic System WGS84 (Fig.1) utilizing two angles and the altitude.

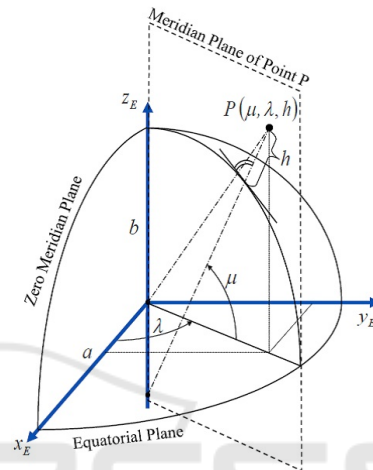


Figure 1: Geodetic system WGS84.

The radius of curvature in the prime vertical  $N_{\mu}$  and the meridian radius of curvature  $M_{\mu}$  are computed from the semi-major axis length  $a$  of the reference ellipsoid and the first eccentricity  $e$ , where the first eccentricity  $e$  has to be calculated from the flattening  $f$ :

$$e^2 = 2f - f^2$$

The flattening  $f$  is defined as:

$$f = \frac{a - b}{a}$$

### 2.5 Tactile Display System Inputs

The Results of (McGrath, 2000) showed that roll and pitch information could be provided by tactile cues via an array of tactors placed in belt which is incorporated into a torso harness. Which means that banking to the left is displayed on a column of tactors on the left side of the torso and vice versa. A display flight paths going down on the abdomen and flight paths going up on the back, to have a clear distinction between going down and up.

But in reality the pilot did not need to perceive the pitch and bank angles during the flight. On the

other hand, the turn rate and the flight path climb angles are two very important informations for the pilot. For more details we suggested to change the horizontal feedback from feeding back the bank angle to feeding back the turn rate angle to give a better sensation of whether the aircraft was veering to the right direction or not (which is not always directly related to the banking angle). And the vertical feedback was changed from feeding back the pitch angle to feeding back the flight-path inclination angle. This is less complex and might be easier to understand. These two variables take into account the aircraft's flight envelope and the optimal recommendation to prevent and avoid the crash plane.

This implementation would require two columns of tactors to display the vertical direction: one on the abdomen and one on the back, and two columns of tactors on each side of the torso to display the horizontal flight path changes.

For the acquisition of the flight-path inclination angle and the turn rate angle we use the aircraft model implemented in Matlab/Simulink environment.

### 2.6 Design of the Tactile Display System

We have developed a tactile display system consisting of 16 vibrating elements (tactors). We used 4 columns of 4 tactors. Each tactor is placed in the box developed by a 3D printer and designed in the Institute of Flight System Dynamics(FSD)/ Technical University Munich of Germany (Fig.2).

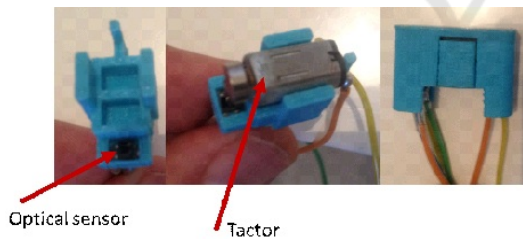


Figure 2: Box of tactor.

The turn rate and the flight path climb angles were encoded using a combination of column selection. For instance, when turn rate left, the column of tactors on the left side of the torso was selected as the load factor was not reached and the bank angle was not in the boundary zone. We follow the same approach and display flight paths going down on the abdomen and flight paths going up to the back, to have a clear distinction between going down and up to avoid confusion the horizon was displayed on the same side as the flight path climb angle. When the airplane was flying level (flight path climb angle equals zero), the flight

path climb angle and the horizon were displayed on both sides, the abdomen and the back. Also the tactor location was used to encode the information for turn rate or flight path climb angle. The range for the horizontal feedback (turn rate) was set to [-6.0, -4.0, -2.0, -0.7, 0.7, 2.0, 4.0, 6.0] degrees per second. For the vertical (flight path climb angle) it was set to [-7.0, -5.0, -3.0, -0.7, 0.7, 3.0, 5.0, 7.0] degrees. We add with these two flight data, turn rate and flight path climb angle, the flight envelope, pitch, flight path climb and bank angles limits to generate a warning signal which warns the pilot of any wrong control. For that, we implemented a fuzzy logic controller block that generates the warning signal or the display of turn rate and flight path climb angles using the following logic.

As long as the limits on the flight envelope, pitch, bank or flight path climb angles are not reached we display the turn rate and the flight path climb angles with the recommended frequency. If the limit of the flight path or pitch angles is reached we activate the eight tactors on the horizontal feedback and if the limit of the bank angle is reached we activate the other eight tactors on the vertical feedback. The limit of the flight envelope involves the activation of all the sixteen tactors with specific frequency.

The used flight data, turn rate, flight path climb, pitch, bank angles and flight envelope must be converted into tactile signals ie intensity and location on the skin by using the fuzzy logic controller (Fig.3).

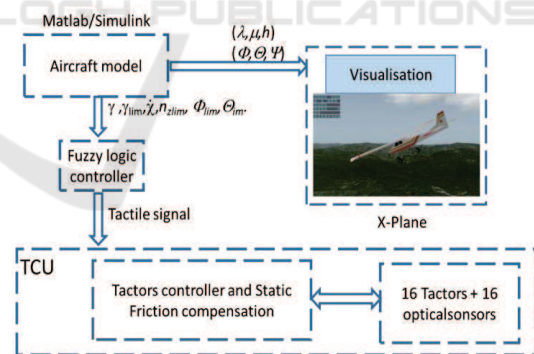


Figure 3: Design of the tactile display system.

As shown in Fig.4 and Fig.5, an ARM Cortex M3 microcontroller forms the core of the Tactile Control Unit (TCU). The modified speed controller implemented on the microcontroller is used for amplitude control, temporal rhythm generation and compensate the static friction. Sixteen interruptions pins of the ARM Cortex M3 are configured to read a frequency of each tactor in the real time. All of the 16 tactors listen to the main controller for specific commands on the amplitude and the timing of vibration through

the I2C bus. The spatial coordinates of a stimulus

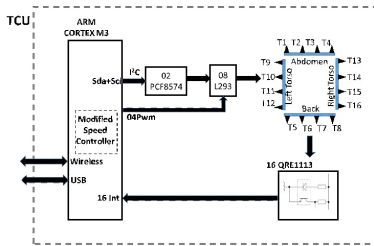


Figure 4: Tactile controller unit schematic.

applied to the skin are accurately represented in the central nervous system, and so it has been proposed that spatial information about the external world may be communicated via tactile stimulation of the skin (Van Veen and Van Erp, 2001). In general, the ability to localize a point of vibrotactile stimulation on the body is best when it is presented near anatomical points of reference such as the wrist, elbow, spine, or navel (Cholewiak et al., 2004). Cholewiak et al. (Cholewiak et al., 2004) determined the number of sites around the waist at which participants could accurately localize vibrotactile stimulation. The tactile array comprised a belt with 12 (intertactor spacing of 72 mm), 8 (spacing of 107 mm), or 6 (spacing of 140 mm) tactors equidistantly spaced. Localization accuracy averaged 74% correct with 12 tactors, and it improved to 92% with 8 tactors and to 97% when 6 tactors were used. In our case the tactors were affixed to the band, with a 107 mm vertical spacing in the torso, and spacing of 100 mm in the abdomen and back. All communications from the fuzzy logic controller or block logic are received through the IEEE 802.15.4 wireless module or USB by the ARM Cortex M3. The data received are automatically used by the modified speed controller to compensate the static friction (Fig.5).

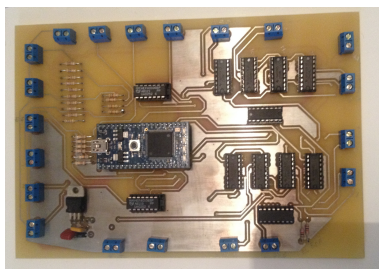


Figure 5: Tactile controller unit.

### 3 TACTILE CONTROLLER UNIT DESIGN

#### 3.1 Modeling, Parameters Identification and Open Loop Experiments on 308-102 Tactors

Tactors are modelled as eccentric rotating mass actuator with an imbalanced load fixed to the radial center axle. The mathematical model of the vibration tactors is given by (Vartholomeos and Papadopoulos, 2006):

$$\ddot{\theta}_t = \frac{K_T}{JR} V_S - \frac{K_T^2}{JR} \dot{\theta}_t - \left( \frac{c}{J} \text{sign}(\dot{\theta}) + \frac{b}{J} \dot{\theta} \right) - \frac{m_t g r}{J} \sin \theta_t \quad (3)$$

Where  $K_T$  is the tactor's torque constant,  $J$  is the inertia of the eccentric load mass,  $R$  is the tactors ohmic resistance,  $r$  is the length between the center of the radial axis and the center of eccentric load mass. the voltage,  $V_S$ , is the input voltage to the actuator, and the angle  $\theta_t$  is the angular position of the tactor with respect to the radial axis. The term  $(\frac{c}{J} \text{sign}(\dot{\theta}_t) + \frac{b}{J} \dot{\theta}_t)$  is the coulomb and viscous friction.

Parameters identification is necessary for the simulation of a tactor dynamics and the design of the controller strategies. Therefore, tactor parameters are determined by recording a set of measurements. Nevertheless, an important constraint prevented from measuring the angular positions by the use of the commercial encoders due to the small dimensions of the tactor. for that, an approach is adopted to overcome the problem of measurement of the angular positions by the implementation and design of an encoder.

The torque constant,  $K_T$  is obtained by measuring the steady state current  $i_{ss}$  through the tactor and its steady state rotational speed  $\omega_{ss}$  from the following equation :

$$K_T = \frac{1}{\omega_{ss}} (V_S - R i_{ss}) \quad (4)$$

The coulomb friction reduces the torque applied by the motor and is dependent on the direction of the velocity. To obtain the coulomb friction we measure the current  $i_s$  necessary to start the tactor. The coulomb friction coefficient  $c$  is :

$$c = i_s K_T \quad (5)$$

The viscous friction coefficient  $b$  is obtained in the steady state by :

$$b = \frac{1}{\omega_{ss}} (i_{ss} K_T - c \text{sign} \omega_{ss}) \quad (6)$$

Then, the total inertia of the tactor,  $J$ , is given by:

$$J = \frac{\tau K_T^2 + R b}{R} \quad (7)$$

Where,  $\tau$ , is the time constant in the open loop response of the equation (3). The identification of the different parameters of the dynamic model were determined as the average of ten series of experiment.

Figure 6 shows the open loop response of rotational speed in simulation and real environment for different values of input (2.9V-4V). We observe from the responses of angular velocity in simulation and real environment in Fig.6 that the model of tactor is successefully identified. However, the time constant is about 40 ms (for more precision see Fig.11). We notice that this time constant is not suitable for the tactile display applications which requires stimulation of about 50 ms. In order to minimize the time constant of the response of tactor a rotational speed controller is designed and implemented in the ARM Cortex M3 microcontroller.

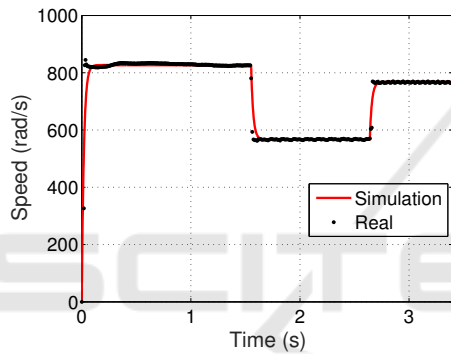


Figure 6: Speed response for different voltage input in open loop.

loop speed response for the desired value 700 rad/s. A presence of overshoot is due to the closed loop zero, and due to the limit power of the LiPo battery with regulator (5V) while the controller requires more voltage (Fig.9). So, in order to overcome the problem of overshoot we modify the strategie of controller.

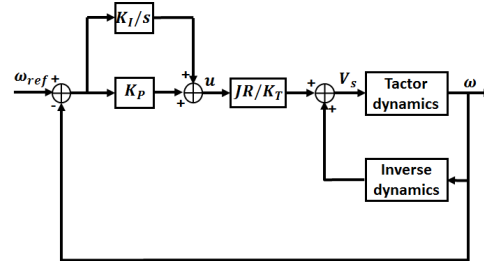


Figure 7: Rotational speed controller design.

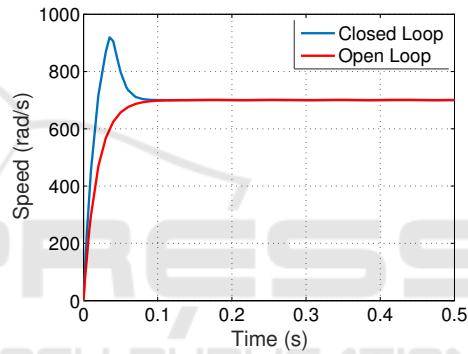


Figure 8: Closed and open loop simulation of speed response.

### 3.2 Speed Controller Design

In this section we are interested to develop a design controller strategie for the tactors to minimize the time constant of the system. The use of batteries to achieve the autonomy, impose restriction that the voltage input can not exceed 5V.

To this aim, the tactor is controlled using inverse dynamics given by:

$$V_s = (K_T^2 + Rb)\omega + Rm_t g r \sin(\omega) + cR K_T^{-1} + \frac{JR}{K_T} u \quad (8)$$

Where  $u$  is actuating signal incorporating in proportional plus integral control:

$$u = K_p(\omega_{ref} - \omega) + K_I \int (\omega_{ref} - \omega) dt \quad (9)$$

The controller is described in Fig.7. The inverse dynamics compensate the two non linear terms. The  $K_p$ ,  $K_I$  eliminate the permanent state error of the tactor's speed and result to a much faster response. Fig.8 shows the comparison between the open and closed

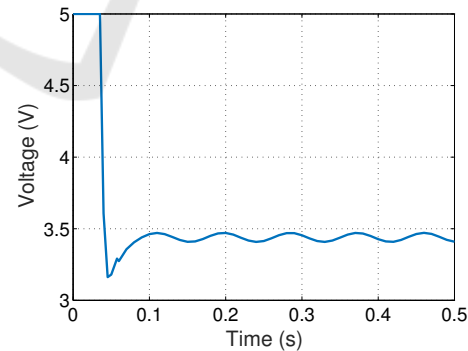


Figure 9: Evolution of the input voltage in closed loop with PI controller.

The modified controller speed is shown in Fig.10, and the actuating signal  $u$  becomes:

$$u = -K_p \omega + K_I \int (\omega_{ref} - \omega) dt \quad (10)$$

The poles of the system designed in Fig.10 are placed

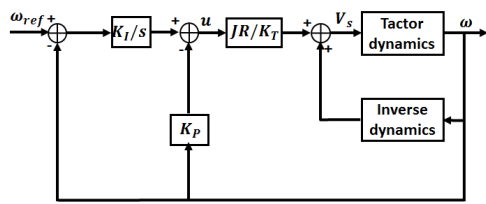


Figure 10: Modified speed controller design.

at the same point to avoid oscillations, ie the damping coefficient is equal to 1, and the settling time  $t_s = 4.7\omega_n$ . Where  $\omega_n$  is the natural frequency. The gain parameters of the speed controller are  $K_p = 354$ , and  $K_I = 31343$  by choosing a desired settling time as  $26.44ms$  under the constraint of the limit voltage of the battery (Lipo + regulator 5v).

Figure 11 shows the response of angular speed of closed loop of the modified speed controller (red line) and open loop simulation (blue line) for a desired speed 700 rad/s. We obtain a reduction of 48% in settling time, ie time constant is equal to 20.8ms. In addition, there is no overshoot in the closed loop modified controller response. Fig.12 shows that the input voltage in the modified controller is under 5V and no saturation is detected during its evolution.

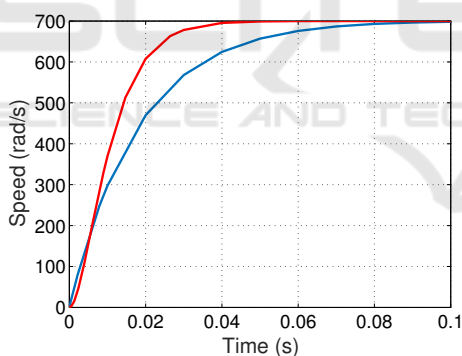


Figure 11: Zoomed modified speed controller and open loop simulation of speed response.

The modified controller is implemented in the ARM CORTEX M3 microcontroller. Eight (08) L293 quadruple half-H drivers was used to drive sixteen tactors. Pulsed Width Modulation (PWM) with the modified speed controller strategie were applied to control the angular speed of the tactors. To measure the rotational speed, a very low cost opto-reflective sensor QRE1113 was used for each tactor. However, the output signal of the opto-reflective sensor is filtered with a shmitt trigger HEF40106BP.

For the experimental procedure, we applied the modified controller presented in equation 9, omitting the term containing the angle of rotation,  $\theta$ . During

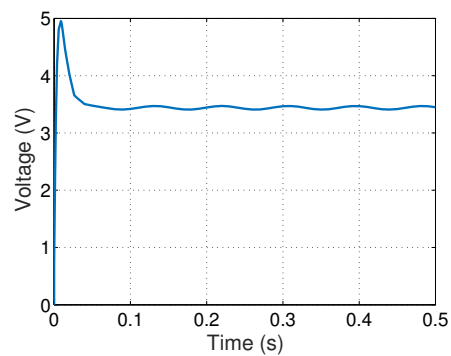


Figure 12: Evolution of the input voltage in modified controller.

the practice it was necessary to use the developed optical encoder QRE1113 as explained in the previous section.

Figure13 shows the response of the real and simulation speed of the tactor for the closed loop with the modified controller. We observe that the steady state error is less than 3% and the time constant is 20.8 ms. The diagram of the developed tactile system is

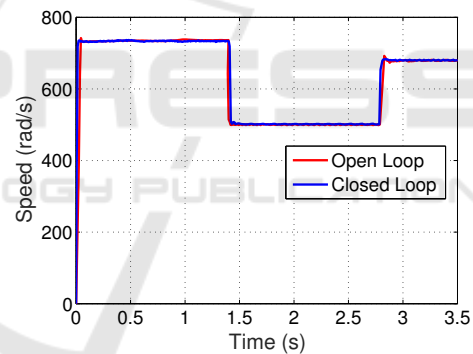


Figure 13: Real and simulation speed response of the modified controller for different voltage inputs.

divided into two parts. The first is the software unit composed of fuzzy logic controller wich is used to transform the flight data to tactile signals. The second part is the hardware unit which consist in reducing the time constant to adapt the low cost tactor to the tactile display applications and control the tactors according the transmitted flight data.

## 4 EXPERIMENTAL EVALUATION

### 4.1 Flight Data Constraints

Flight data constraints are used to check the limits of the flight envelope, pitch, bank or the flight path climb

angles and activate the embedded tactile display system in the real time.

Most operating limitations can be translated to limits other parameters. Enforcing the speed limits can be impossible if the pilot has full authority over the vertical motion of an aircraft. In this case only the throttle could be used by the flight control system for speed protection purposes. This is evidently no sufficient for an effective protection when aircraft is in steep climb or descent. Hence, it makes sense to translate the speed limits to the flight path climb angle limits. Equation ((11)) shows how the speed rate is related to the flight path climb angle.

$$\dot{V}_k = g(n_x)_k - g \sin \gamma_k \quad (11)$$

The speed rate can be limited depending on the current indicated airspeed and the limit indicated airspeed ; as in equation (12) with a constant k (Zhang et al., 2014).

$$\dot{V}_{lim} = k(V_{lim} - V_k) \quad (12)$$

By simple rewriting of equation (12), the upper and lower limits on the flight path climb angle can be written as in equations (13) and (14).

$$\gamma_{lim,U} = \arcsin\left((n_x)_k - \frac{k(V_{lim,U} - V_k)}{g}\right) \quad (13)$$

$$\gamma_{lim,L} = \arcsin\left((n_x)_k - \frac{k(V_{lim,L} - V_k)}{g}\right) \quad (14)$$

Where  $V_{lim,U}$  is the never exceed speed  $V_{NE}$  and  $V_{lim,L}$  is the stall speed  $V_{stall}$  (Fisch et al., 2012). The bank angle limitation is a function of height above terrain (equation (15)). When the aircraft center of gravity is at or below 2m above terrain; the wings level attitude is imposed. At higher altitudes, the bank angle limit linearly increases to 15m, i.e., at the end of take-off or at beginning of landing,  $20^0$  are allowed.

$$\Phi_{lim,h} = \begin{cases} 0 & \text{if } x \leq 2m \\ 20^0 \frac{h-2m}{13m} & \text{if } x > 2m \end{cases} \quad (15)$$

To prevent excessive attitudes, the following limits on pitch and bank angle are imposed.

$$\Phi_{lim,U} = 60^0$$

$$\theta_{lim,U} = 20^0$$

$$\theta_{lim,L} = -10^0$$

## 4.2 Fuzzy Logic Controller

The architecture of the tactile display system use a Fuzzy Logic Controllers (FLC), to controls vibration frequency, timing and location, from which vibrotactile spatiotemporal patterns can be created. One main

characteristic of a fuzzy controller is its applicability to systems with uncertainty or even with unknown models (Sepehri and Lawrence, 1998). This makes a fuzzy controller ideal for dynamically reproducing the multimodal aerodynamic display of the flight data parameters with the flight envelop and the optimal decision in the torso and abdomen of the pilot.

This part focuses on design of a Mamdani fuzzy model which shall generate adequate duration, location and frequency of each factors based on the aerodynamic data (see Fig.5). The fuzzy controller was designed to account for the different parameters those affect the horizontal and vertical flight path changes. The stability aspect of the outer loop including the fuzzy model is not addressed in this work and more details about the design of fuzzy controllers can be found in (Jantzen, 1998).

Six variables were used as input for fuzzy controller those are, the flight envelope limit, turn rate, the flight path climb, pitch limit, bank limit and flight path climb limit angles. The outputs of FLC are the desired frequency and location of factors in horizontal and lateral directions. To define the outputs we need to understand the behaviour of the skin and the amplitudes required for frequency of stimulation and rhythm. So, The Optimal sensitivity is achieved at frequencies between 25 and 320 Hz for abdomen site (Cholewiak et al., 2004). Furthermore, in most tactile displays, people prefer that the duration of the tactile pulses has to be between 20 and 320 ms (optimally near 50 ms), and when the tactile display is functioning as a simple alert the duration has to be between 50 and 200 ms (Kaaresoja and Linjama, 2005). In our work, we created a rhythms together so as to group vibrotactile pulses of varying durations (Brown et al., 2005). In which we used a duration of 50 ms with flight path climb and turn rate angles data display, a duration of 150 ms to indicate alerts to keep the aircraft in its flight envelope. The linguistic terms of each input variable are defined as follows:

**Flight Path Climb Angle:** NVBG (Negative Very Big Gamma), NBG (Negative Big Gamma), NMG (Negative Medium Gamma), NSG (Negative Small Gamma), ZG (Zero Gamma), PSG (Positive Small Gamma), PMG (Positive Medium Gamma), PBG (Positive Big Gamma), PVBG (Positive Very Big Gamma).

**Turn Rate Angle:** NVBT (Negative Very Big Turn), NBT (Negative Very Big Turn), NMT (Negative Medium Turn), NST (Negative Small Turn), ZT (Zero Turn), PST (Positive Small Turn), PMT (Positive Medium Turn), PBG (Positive Big Turn), PVBG (Positive Very Big Turn).

**Pitch Limit:** NLP (No Limit Pitch), LP (Limit Pitch).

**Bank Limit:** NLB (No Limit Bank), LB (Limit Bank).

**Flight Path Climb Angle Limit:** NLG (No Limit Gamma), LG (Limit Gamma).

**Flight Envelope Limit:** NLE (No Limit Envelope), LE (Limit Envelope).

Once the proper inputs were created, the next step is to create the output characteristic behavior of the tactile signal being received by the TCU unit. The outputs variables Vibration characteristics (Location/Frequency/Timing) was classified as :

**Vertical Tactor:** VBT8 (Vertical Back Tactor 8), VBT7 (Vertical Back Tactor 7), VBT6 (Vertical Back Tactor 6), VBT5 (Vertical Back Tactor 5), ZVT (Zero Vertical Tactor), VAT1 (Vertical Abdomen Tactor 1), VAT2 (Vertical Abdomen Tactor 2), VAT3 (Vertical Abdomen Tactor 3), VAT4 (Vertical Abdomen Tactor 5), VLT (Vertical Limit Tactors).

**Side Tactor:** RST8 (Right Side Tactor 8), RST7 (Right Side Tactor 7), RST6 (Right Side Tactor 6), RST5 (Right Side Tactor 5), ZST (Zero Side Tactor), LST1 (Left Side Tactor 1), LST2 (Left Side Tactor 2), LST3 (Left Side Tactor 3), LST4 (Left Side Tactor 5), SLT (Side Limit Tactors).

The next step is to create a rule base that would govern the operation of the fuzzy controller. Proper conditions must be created in order to implement a system that will display the flight data and secure the flight. In order to establish such a collection of fuzzy rules, we questioned experts (pilots), using a carefully organized questionnaire and to complete the rules table system as shown in Table 1. The use of expert knowledges is the most common approach to design fuzzy controller rules and convert the flight data on tactile signals.

Figures (14), (15), (16), (17), (18),(19), (20) and (21) show an example of simulated manoeuvres for a model aircraft. Fig.14 shows the evolution of the pitch and the bank angles and Fig.15 shows the historical time of the normal load factor and the limits of the normal load factor according to the airspeed. Fig.16 shows the historical time of the flight path climb angles and its upper and lower limits while Fig.17 represents the location of each tactor in the abdomen site. In this figure we find the activation of the tactors T1, T2, T3, T4 according to the value of the flight path climb angle. After 47 sec the flight climb angle approach the upper limit (Fig.16) and the four tactors are activated during this period to display the warning signal of the limit approach. This limit will cause an approach towards the limit of the flight envelope for 14 sec (Fig.17). During this period the pilot is informed of this situation by the tactile signal and tries to avoid this approach by the action on the control

stick by decreasing the flight path climb angle. These limits will activate all the eight tactors of the horizontal site (Fig.18). We notice that the tactors are activated during the flight to inform the pilot about the flight path climb angle by using the tactile display.

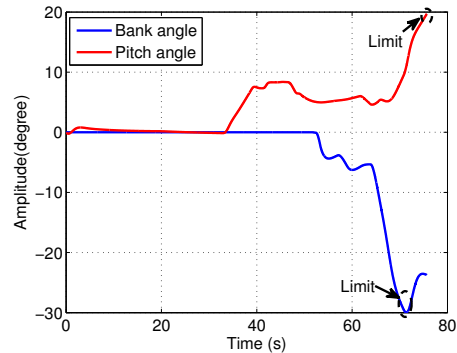


Figure 14: Pitch and bank angles limit.

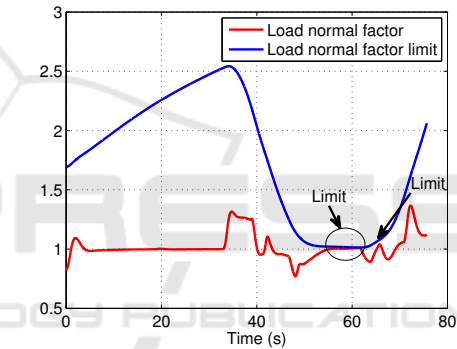


Figure 15: Load factor limit.

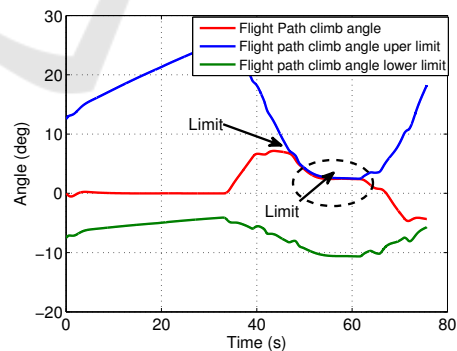


Figure 16: Flight path climb angle limit.

Figures (19) and (20) show the tactors activation on the right and left side. In Fig.19 the tactors are activated only in the two limit of the flight envelope (Fig. 15) and the limit of bank angle according to the time of 70sec (Fig.14). While Fig.20 show the activation of the tactors when the pilot actuate the stick to turn left. The limits of flight envelope and bank angle

Table 1: Rule base system.

$\Delta n_{z,lim}/\theta_{lim}$ $\gamma/\gamma_{lim}$	NVBG/ NLG	NBG/ NLG	NMG/ NLG	NSG/ NLG	ZG/ NLG	PSG/ NLG	PMG/ NLG	PBG/ NLG	PVBG / NLG
NLE/Nolimit	VBT8	VBT7	VBT6	VBT5	ZVT	VAT1	VAT2	VAT3	VAT4
NLE/Limit	VLT	VLT	VLT	VLT	VLT	VLT	VLT	VLT	VLT

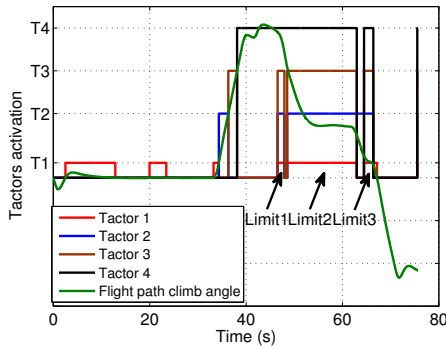


Figure 17: Tactores activation on the abdomen site.

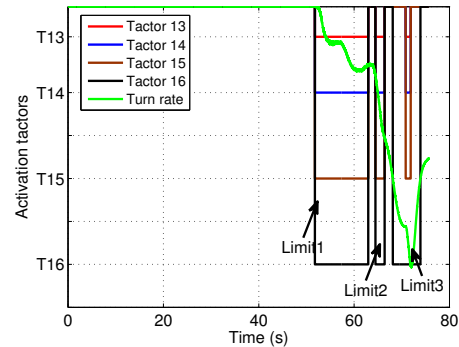


Figure 20: Tactores activation on the left side site.

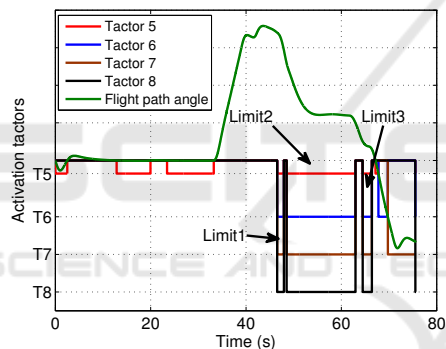


Figure 18: Tactores activation on the back site.

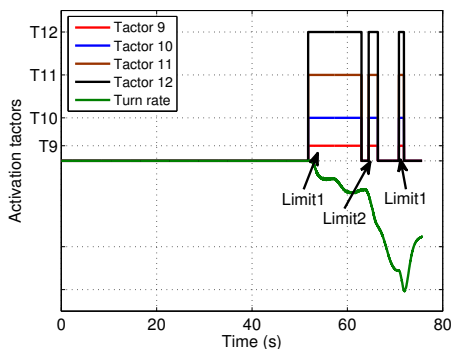


Figure 19: Tactores activation on the right side site.

When the pilot actuat commands a positive pitch by deflecting the sidestick at the time of 33sec the aircraft climbs. This action also increase the flight path climb angle and the frequency of T1 is 320 Hz at 34 sec, T2 is 320 Hz at 36 sec, T3 is 320 Hz at 38 sec and T5 is 270Hz at 40 sec.

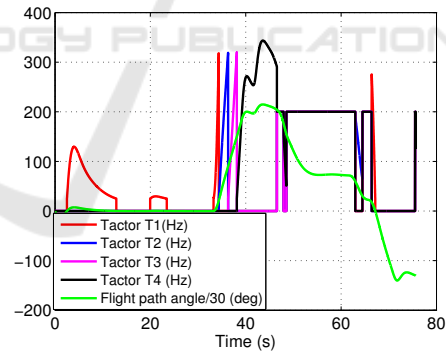


Figure 21: Frequency factors on the abdomen site.

are respected by generating the warning signal.

Fig.21 shows the frequency of factors on the abdomen site calculated from the output signal of the fuzzy logic controller. The maximum of frequency correspond to 320Hz and the minimum is 25 Hz.

## 5 CONCLUSION

This paper reports a successful achievement of a new hardware/software controller for realisation of tactile display system used in the cockpit design. The assembled prototype and the related built-in software have been integrated successfully with a dynamic model of an aircraft and commercial software that assure the aircraft visualization. In order to achieve a successful transformation of a flight data to tactile signal fea-

tures, we have implemented a knowledge based fuzzy system which allows deriving the amount of vibration to be reproduced on the mechanoreceptor in the pilot skin. The designed controller imitates the real features of tactile display and allows the pilot's central nervous. Also for the flight data and warning signals to control a virtual aircraft in stressed situations. Experiments were performed in order to evaluate the proposed control loop based on a modified speed controller with a fuzzy logic controller. This idea is a step to use the low cost tactors in the tactile display field by reducing the settling time in comparison to the open loop response and delete the overshoot. our own flexible tactile display can be reconfigured or dynamically changed to inject different flight data or simulate different parts of the skin.

## REFERENCES

- Arasan, A., Basdogan, C., and Sezgin, T. M. (2013). Haptic stylus with inertial and vibro-tactile feedback. In *World Haptics Conference (WHC), 2013*, pages 425–430. IEEE.
- Brown, L. M., Brewster, S. A., and Purchase, H. C. (2005). A first investigation into the effectiveness of tactons. In *Eurohaptics Conference, 2005 and Symposium on Haptic Interfaces for Virtual Environment and Teleoperator Systems, 2005. World Haptics 2005. First Joint*, pages 167–176. IEEE.
- Brown, L. M. and Kaaresoja, T. (2006). Feel who's talking: using tactons for mobile phone alerts. In *CHI'06 extended abstracts on Human factors in computing systems*, pages 604–609. ACM.
- Choi, S. and Kuchenbecker, K. J. (2013). Vibrotactile display: Perception, technology, and applications. *Proceedings of the IEEE*, 101(9):2093–2104.
- Cholewiak, R. W., Brill, J. C., and Schwab, A. (2004). Vibrotactile localization on the abdomen: Effects of place and space. *Perception & Psychophysics*, 66(6):970–987.
- Cholewiak, R. W. and Collins, A. A. (2003). Vibrotactile localization on the arm: Effects of place, space, and age. *Perception & psychophysics*, 65(7):1058–1077.
- Erp, V., Jan, B., Veltman, J., van Veen, H., and Oving, A. (2003). Tactile torso display as countermeasure to reduce night vision goggles induced drift. Technical report, DTIC Document.
- Feng, G. (2006). A survey on analysis and design of model-based fuzzy control systems. *Fuzzy systems, IEEE Transactions on*, 14(5):676–697.
- Fisch, F., Lenz, J., Holzapfel, F., and Sachs, G. (2012). On the solution of bilevel optimal control problems to increase the fairness in air races. *Journal of Guidance, Control, and Dynamics*, 35(4):1292–1298.
- Jansen, C., Wennemers, A., Vos, W., and Groen, E. (2008). *Flytact: A tactile display improves a helicopter pilots landing performance in degraded visual environments*. Springer.
- Jantzen, J. (1998). Tuning of fuzzy pid controllers. *Technical University of Denmark, report*.
- Jiang, T. and Li, Y. (1996). Generalized defuzzification strategies and their parameter learning procedures. *Fuzzy Systems, IEEE Transactions on*, 4(1):64–71.
- Jones, L. A. and Sarter, N. B. (2008). Tactile displays: Guidance for their design and application. *Human Factors: The Journal of the Human Factors and Ergonomics Society*, 50(1):90–111.
- Kaaresoja, T. and Linjama, J. (2005). Perception of short tactile pulses generated by a vibration motor in a mobile phone. In *Eurohaptics Conference, 2005 and Symposium on Haptic Interfaces for Virtual Environment and Teleoperator Systems, 2005. World Haptics 2005. First Joint*, pages 471–472. IEEE.
- Kapur, P., Jensen, M., Buxbaum, L. J., Jax, S. A., and Kuchenbecker, K. J. (2010). Spatially distributed tactile feedback for kinesthetic motion guidance. In *Haptics Symposium, 2010 IEEE*, pages 519–526. IEEE.
- Kelley, A. M., Cheung, B., Lawson, B. D., Rath, E., Chirasson, J., Ramiccio, J. G., and Rupert, A. H. (2013). Efficacy of directional cues from a tactile system for target orientation in helicopter extractions over moving targets. Technical report, DTIC Document.
- Lawson, B. D. and Rupert, A. H. (2014). Coalition warfare program tactile situation awareness system for aviation applications: System development. Technical report, DTIC Document.
- Lloyd, D. M., Merat, N., Mcglone, F., and Spence, C. (2003). Crossmodal links between audition and touch in covert endogenous spatial attention. *Perception & Psychophysics*, 65(6):901–924.
- McGrath, B. J. (2000). Tactile instrument for aviation. Technical report, DTIC Document.
- Nojima, T. and Funabiki, K. (2005). Cockpit display using tactile sensation. In *null*, pages 501–502. IEEE.
- Petit, G. (2013). *Conception, prototypage et évaluation dun système pour l'exploration audio-tactile et spatiale de pages web par des utilisateurs non-voyants*. PhD thesis, École Polytechnique de Montréal.
- Precup, R.-E. and Hellendoorn, H. (2011). A survey on industrial applications of fuzzy control. *Computers in Industry*, 62(3):213–226.
- Renwick, K. (2008). Effectiveness of vibration-based haptic feedback effects for 3d object manipulation.
- Rosenblum, L. D. (2011). *See what I'm Saying: The Extraordinary Powers of Our Five Senses*. WW Norton & Company.
- Sala, A., Guerra, T. M., and Babuška, R. (2005). Perspectives of fuzzy systems and control. *Fuzzy Sets and Systems*, 156(3):432–444.
- Salzer, Y. and Oron-Gilad, T. (2015). Evaluation of an on-high vibrotactile collision avoidance alerting component in a simulated flight mission. *Human-Machine Systems, IEEE Transactions on*, 45(2):251–255.
- Schmidt-Skipiol, F. J. (2015). Tactile feedback and situation awareness.
- Seiderman, A., Marcus, S. E., and Hapgood, D. (1989). *20/20 is not enough: the new world of vision*. Alfred A. Knopf.

- Self, B., Van Erp, J. B., Eriksson, L., and Elliott, L. (2008). Human factors issues of tactile displays for military environments. *Tactile Displays for Orientation, Navigation and Communication in Air, Sea and Land Environments*, pages 1–18.
- Sepehri, N. and Lawrence, P. D. (1998). Fuzzy logic control of a teleoperated log loader machine. In *Intelligent Robots and Systems, 1998. Proceedings., 1998 IEEE/RSJ International Conference on*, volume 3, pages 1571–1577. IEEE.
- Tang, F., McMahan, R. P., and Allen, T. T. (2014). Development of a low-cost tactile sleeve for autism intervention. In *Haptic, Audio and Visual Environments and Games (HAVE), 2014 IEEE International Symposium on*, pages 35–40. IEEE.
- Thomas, P., Biswas, P., and Langdon, P. (2015). State-of-the-art and future concepts for interaction in aircraft cockpits. In *Universal Access in Human-Computer Interaction. Access to Interaction*, pages 538–549. Springer.
- Van Erp, J. and Self, B. (2008). Introduction to tactile displays in military environments. *Tactile Displays for Orientation, Navigation and Communication in Air, Sea, and Land Environments*, pages 1–1.
- Van Erp, J. B., Van Veen, H. A., Jansen, C., and Dobbins, T. (2005). Waypoint navigation with a vibrotactile waist belt. *ACM Transactions on Applied Perception (TAP)*, 2(2):106–117.
- Van Veen, H. A. and Van Erp, J. B. (2001). Tactile information presentation in the cockpit. In *Haptic Human-Computer Interaction*, pages 174–181. Springer.
- van Wassenhove, V. (2009). Minding time in an amodal representational space. *Philosophical Transactions of the Royal Society of London B: Biological Sciences*, 364(1525):1815–1830.
- Vartholomeos, P. and Papadopoulos, E. (2006). Analysis, design and control of a planar micro-robot driven by two centripetal-force actuators. In *Robotics and Automation, 2006. ICRA 2006. Proceedings 2006 IEEE International Conference on*, pages 649–654. IEEE.
- Wellman, P. S., Peine, W. J., Favalora, G., and Howe, R. D. (1998). Mechanical design and control of a high-bandwidth shape memory alloy tactile display. In *Experimental robotics V*, pages 56–66. Springer.
- Zhang, F., Braun, S., and Holzapfel, F. (2014). Physically integrated reference model and its aids in validation of requirements to flight control systems. In *AIAA Guidance, Navigation and Control Conference*, pages 2014–0962.